

Hybrid Structural Control of the 20-Story Benchmark Structure

¹Pham Nhan Hoa, ²Chu Quoc Thang

¹Department of Civil Engineering, International University - Vietnam National University-HCM

²Department of Civil Engineering, International University - Vietnam National University-HCM

¹pnhoa@hcmiu.edu.vn, ²cqthang@hcmiu.edu.vn

ABSTRACT

The paper presents the multi-story structures equipped with a hybrid control system in attempts to improve seismic resistance. A hybrid control system consists of semi-active controlled stiffness devices (CSD) and additional passive controlled fluid viscous dampers (VFD) to obtain higher capability control force produced by both of the dampers for an optimal structural response. Four active control algorithms (Riccati Optimal Active Control Algorithm, Instantaneous Control with Displacement and Velocity Feedback, Instantaneous Optimal Active Closed-Loop Control Algorithm, and Pole Placement Algorithm) are used to control the CSD of the structure. Focusing on a steel structure which is the benchmark 20-story building designed for the SAC project for the Los Angeles, California, the numerical example analyzes the dynamic response of the building controlled with the hybrid system and subjected to earthquake-induced motion. Also, the effectiveness of response reduction in the building equipped with combined devices are significantly better compared to the uncontrolled structure, the structure with only passive VFD, and with semi-active CSD. Finally, in the conclusion we discuss some advantages of the hybrid control system for seismic resistance in Vietnam.

Keywords: Dynamics of Structures, Structural Control, Dampers, Hybrid Control, Viscous Fluid Dampers, Controlled Stiffness Devices

1. INTRODUCTION

The hybrid control has economic advantages compared to the passive control and semi-active control. It is passive dissipaters that are responsible for seismic resistance to a weak earthquake and semi-active devices that are in charge of resisting a strong earthquake. Consequently, energy for a structure in attempts to mitigate the dynamic responses of the structure is required reasonably. Mixing both a controlled stiffness device and a fluid viscous damper into one brace is {1} to employ the strong points of both VFD and CSD, {2} to utilize the force generated from both of them during motion, {3} to simultaneously create a passive and semi-active controllable system. Furthermore, derived from the study in the field of structural control involving buildings equipped with only viscous fluid dampers (VFD) [3] or only controlled stiffness devices (CSD) [5], CSDs can be rapidly semi-active controlled but their drawback is the capability of producing variable force while VFDs is difficult creating a semi-active system. Control forces generated by VFD or CSD depend on the motion of two adjacent story. In fact, the internal features of the VFD involve the flow of compressible silicon oil through specially designed passages located in and around the piston head. As opposed to CSD, a passive viscous damper force generated by VFD at the i^{th} floor is given by [3]

$$F_i^{VFD}(t) = C_i^{VFD} |\dot{x}_i(t) - \dot{x}_{i-1}(t)|^r \text{sign}[\dot{x}_i(t) - \dot{x}_{i-1}(t)] \quad (1)$$

where C_i^{VFD} is the damping coefficient; $\dot{x}_i(t)$ is the velocity at the i^{th} floor; α is a predetermined exponent. Usually for seismic application, $r \approx 1$, producing linear response. Otherwise, the variable force developed by the semi-active controlled stiffness devices at the i^{th} floor is given by [5]

$$u_i^{CSD}(t) = u_i^M + F_i^C \quad (2)$$

$$\left\{ \begin{array}{l} u_i^M = C_i^M [x_i(t) - x_{i-1}(t) + x_i^{ctr}(t)] \\ F_i^C = n_c C_c \left\{ x_0 - [x_i(t) - x_{i-1}(t)] \right\} \left[\frac{\frac{a^2}{4} + x_0^2}{\sqrt{\frac{a^2}{4} + \{x_0 - [x_i(t) - x_{i-1}(t)]\}^2}} - 1 \right] \right\}$$

where C_i^M and C_c are the stiffness coefficients of the main spring and the corrector, respectively; n_c is the number of stiffness correctors; $x_i(t)$ is the displacement; $x_i^{ctr}(t)$ is the displacement of the activating bar at i^{th} floors; x_0 is the horizontal projection of the corrector in the unloaded state; a is the diameter of the internal cylinder.

Due to the properties of CSD, the displacement of the main spring is in elastic domain, therefore $x_i^{ctr}(t)$ must satisfy

$$x_{\text{limit},i}^c \leq x_i[k] - x_{i-1}[k] + x_i^{ctr}(t) \leq x_{\text{limit},i}^t \quad (3)$$

where $x_{\text{limit},i}^c$ and $x_{\text{limit},i}^t$ are compression and tension elastic limit at the i^{th} floor, respectively. The value of C_i^M , $x_{\text{limit},i}^c$ and $x_{\text{limit},i}^t$ are taken from manufactures of CSD. A semi-active controlled force of CSD depends on the magnitude of both main spring's stiffness coefficient and compression and tension limit. The force is quite low compared to a structure's control force needed. Unlike an active control, the control computer determines the displacement of activating bar to produce the semi-active

force vector $u_i^{CSD}(t)$, instead of the active force vector $\hat{u}_i(t)$. The determination of $x_i^{cr}(t)$ is related to the feedback control law obtained from control algorithms. In this paper four active control algorithms applied to calculate $u_i^{CSD}(t)$ consist of Riccati Optimal Active Control Algorithm (ROAC), Pole Placement Algorithm (PPA), Instantaneous Control with Displacement and Velocity Feedback (ICDVF), and Instantaneous Optimal Active Closed-Loop Control Algorithm (IOAC). Eventually, the system combines the forces produced by the semi-active CSD and the additional passive VFD at the i^{th} arbitrary floor:

$$u_i(t) = F_i^{VFD}(t) + u_i^{CSD}(t) \quad (4)$$

The smart structures are assumed {1} to be shear building so that each floor is modeled as a degree of freedom where the mass is concentrated at each floor and the stiffness is provided by columns and {2} to be able to retain elastic and columns' linear behavior under the earthquake. From these assumptions, a n-story multi-bay shear building is associated with a n-story single-bay building as shown in the

Fig 1 and the stiffness coefficient at the i^{th} floor of the shear building ($i=1, 2, \dots, n$) can be calculated with the following expression [2]

$$k_i = \sum_{\text{columns}} \frac{12EI_c}{H^3} \quad (5)$$

where E is the Young's modulus, I_c is the moment of inertia of the columns; H is the length of one column at the i^{th} floor.

On purpose of assessing the effectiveness of response reduction, a reliable model of a controllable structure attaching with the hybrid system of (VFD+CSD) is required to establish the differential equation of motion, subsequently an algorithm to solve this equation. The goal of numerical examples is to estimate the effectiveness in reducing dynamic responses of the benchmark 20-story structure simultaneously equipped with VFD and CSD. This result is compared to such a structure with no control, with only passive VFD, semi-active CSD, and with a classical solution which increases the columns' stiffness of a structure.

2. A SMART STRUCTURE CONTROLLED WITH HYBRID CONTROL

2.1 The Governing Differential Equation of Motion

Consider a n-story single-bay shear building structure subjected to lateral forces and seismic excitations equipped with r dampers (VFD+CSD) at certain floors as shown in

Fig 1, and m_i is the mass; $P_i(t)$ is the lateral force at the i^{th} floor; $w(t)$ is the vector of the ground accelerations. From free-body diagram depicted in Fig 2, the motion equation of such a smart structure under seismic excitations can be expressed in matrix form as

$$\mathbf{M}\ddot{\mathbf{x}} + \mathbf{C}\dot{\mathbf{x}} + \mathbf{K}\mathbf{x} = \mathbf{F}_d\mathbf{u} - \mathbf{M}\mathbf{r}\mathbf{w} \quad (6)$$

where $\mathbf{M} = \begin{bmatrix} m_1 & 0 & 0 & 0 & 0 \\ 0 & \dots & 0 & 0 & 0 \\ 0 & 0 & m_i & 0 & 0 \\ 0 & 0 & 0 & \dots & 0 \\ 0 & 0 & 0 & 0 & m_n \end{bmatrix}$,

$\mathbf{K} = \begin{bmatrix} k_1 + k_2 & -k_2 & 0 & 0 & 0 \\ 0 & \dots & 0 & 0 & 0 \\ 0 & -k_i & k_i + k_{i+1} & -k_{i+1} & 0 \\ 0 & 0 & 0 & \dots & 0 \\ sym & 0 & 0 & -k_n & k_n \end{bmatrix}$ are the constant

mass stiffness matrices, respectively; and \mathbf{C} is the coefficient damping matrix and is determined with the help of Rayleigh method [2]; $\mathbf{r} = [1 \dots 1 \dots 1]^T$; \mathbf{F}_d is the matrix indicating the position of (VFD+CSD); $\mathbf{x} = [x_1 \dots x_i \dots x_n]^T$; $\dot{\mathbf{x}} = \frac{d}{dt}\mathbf{x}$; $\ddot{\mathbf{x}} = \frac{d^2}{dt^2}\mathbf{x}$ are the displacement, velocity, and acceleration vectors of time, respectively;

$$\mathbf{u}(t) = \{P_1(t) - u_1 + u_2, \dots, P_i(t) - u_j + u_{j+1}, \dots, P_n(t) - u_r\}^T$$

is force vector of time, where u_j is the combined force provided by the (VFD+CSD) and calculated with (4) ($j = 1, 2, \dots, r$).

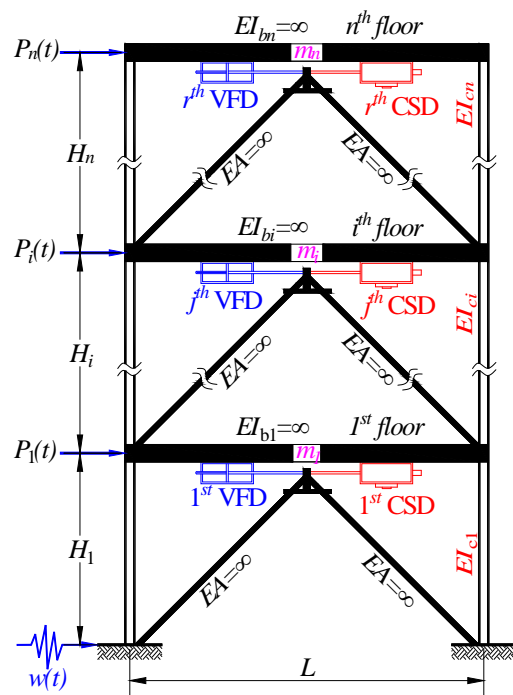


Fig 1: Multi-Story Building equipped with (VFD+CSD) modeled as shear building

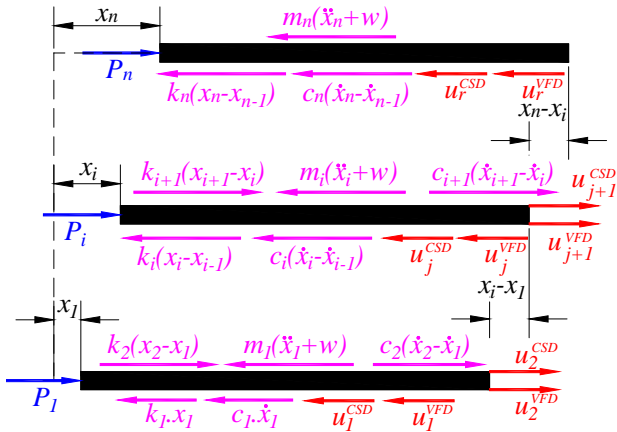


Fig 2: The free body diagram for structures with (VFD+CSD)

2.2 Feature of a Structure With (VFD+CSD)

Consider a seismic structure equipped with the multiple (VFD+CSD) as shown in Fig 3. For the hybrid structural system subjected to a seismic force, as shown in Fig 3, the motion of the system may be rewritten in a state space equation

$$\dot{z}(t) = \mathbf{A} \cdot \mathbf{z}(t) + \mathbf{B} \cdot \mathbf{u}(t) + \mathbf{E} \cdot w(t) \tag{7}$$

where the vector $\mathbf{z}(t) = \begin{Bmatrix} \mathbf{x}(t) \\ \dot{\mathbf{x}}(t) \end{Bmatrix}$ represents the state of the structure which contains the relative-to-ground velocities $\dot{\mathbf{x}}(t)$ and displacements $\mathbf{x}(t)$ of the structure;

$\dot{z}(t) = \frac{dz}{dt}$; $\mathbf{A} = \begin{bmatrix} \mathbf{0} & \mathbf{I} \\ -\mathbf{M}^{-1} \cdot \mathbf{K} & -\mathbf{M}^{-1} \cdot \mathbf{C} \end{bmatrix}$ denotes the system matrix composed of the structural mass, damping and stiffness matrices;

$\mathbf{B} = \begin{bmatrix} \mathbf{0} \\ \mathbf{M}^{-1} \cdot \mathbf{F}_d \end{bmatrix}$ is the distribution matrices of the control forces;

$\mathbf{E} = \begin{bmatrix} \mathbf{0} \\ -r \end{bmatrix}$ is the seismic excitations.

The responses of a structure with hybrid control system is determined with the help of {1} the algorithm zero order hold (ZOH) [1] and {2} the active control law for CSD. After receiving the active control law, the controller block in this system calculates the displacement of the activating bar or producing a semi-active control force. In other words, it is an active control force that decides on how a hybrid controllable structure responds.

Fig 4 depicts the block diagram of a system controlled by the (VFD+CSD). The Closed-loop feedback control is used in this paper and thus the active controlled force matrix can be expressed as:

$$\hat{\mathbf{u}}(t) = -\mathbf{F} \cdot \mathbf{z}(t) \tag{8}$$

where \mathbf{F} is matrix of feedback gain Four algorithms to determine the matrix \mathbf{F} are exhibited in the following subsections.

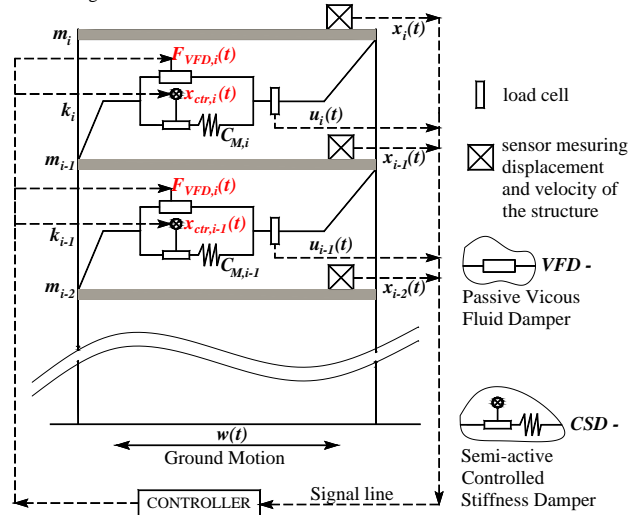


Fig 3: Schematic diagram of a structure with (VFD+CSD) and hybrid control system

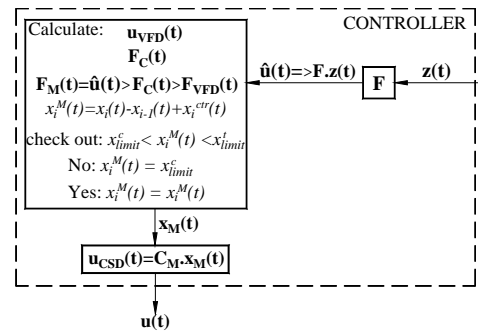


Fig 4: Controller block

2.3 Determining the Active Feedback Gain [1]

2.3.1 Riccati Optimal Active Control Algorithm (ROAC)

In the Riccati optimal algorithm, the control force $\hat{\mathbf{u}}(t)$ may be determined by minimizing a standard quadratic index J , given by:

$$J = \frac{1}{2} \int_{t_0}^{t_f} \left[\mathbf{z}(t)^T \mathbf{Q} \mathbf{z}(t) + \hat{\mathbf{u}}(t)^T \mathbf{R} \hat{\mathbf{u}}(t) \right] dt \tag{9}$$

where \mathbf{Q} is a positive semi-definite symmetrical matrix; \mathbf{R} is an positive-definite symmetrical matrix so that all control forces are effective; performance index, J , represents a weighted balance between structural response and control energy. According to mechanic meaning, J is the energy the structure consume during the earthquake period.

In accordance with [1], the Riccati equation:

$$\mathbf{P} \mathbf{A} + \mathbf{A}^T \mathbf{P} - \mathbf{P} \mathbf{B} \mathbf{R}^{-1} \mathbf{B}^T \mathbf{P} + \mathbf{Q} = 0 \tag{10}$$

Riccati matrix \mathbf{P} in this equation is constant and can be easily solved by numerical methods. Then, the active control expressed by Equation (8) becomes:

http://www.ejournalofscience.org

$$\hat{\mathbf{u}}(t) = -\mathbf{R}^{-1}\mathbf{B}^T\mathbf{P}\mathbf{z}(t) = -\mathbf{F}\mathbf{z}(t) \tag{11}$$

where $\mathbf{F} = \mathbf{R}^{-1}\mathbf{B}^T\mathbf{P}$ (12)

2.3.2 Instantaneous Control with Displacement and Velocity Feedback (ICDVF)

The feedback gain is given in a concise matrix form as

$$\mathbf{F} = \mathbf{B}_2^{-1} \left[\mathbf{z}_c \cdot \text{diag}(\lambda_i)_c - \mathbf{A}_2 \cdot \mathbf{e}_c \right] \cdot (\mathbf{C}_c \cdot \mathbf{e}_c)^{-1} \tag{13}$$

where the diagonal matrix $\text{diag}(\lambda_i)_c$ and the rectangular matrix Φ_c contain the target eigenvalues and eigenvectors, respectively. The matrices \mathbf{A}_2 , \mathbf{B}_2 and \mathbf{z}_c are the lower portions of the matrices \mathbf{A} , \mathbf{B} and \mathbf{e}_c ; \mathbf{C}_c denotes the sensor placement matrix.

2.3.3 Instantaneous Optimal Active Closed-Loop Control Algorithm (IOAC)

In the IOAC algorithm, the optimal control force $\mathbf{u}(t)$ is determined by minimizing an instantaneous time-dependent performance index $J_p(t)$ rather than ROAC integral performance index J:

$$J_p(t) = \mathbf{z}(t)^T \mathbf{Q} \mathbf{z}(t) + \hat{\mathbf{u}}(t)^T \mathbf{R} \hat{\mathbf{u}}(t) \tag{14}$$

The optimal control force $\hat{\mathbf{u}}(t)$ depends on in the time interval Δt , $t_0 \leq t \leq t_f$ and is given by

$$\hat{\mathbf{u}}(t) = -\left(\frac{\Delta t}{2}\right) \mathbf{R}^{-1}\mathbf{B}^T\mathbf{Q}\mathbf{z}(t) = -\mathbf{F}\mathbf{z}(t) \tag{15}$$

where $\mathbf{F} = \left(\frac{\Delta t}{2}\right) \mathbf{R}^{-1}\mathbf{B}^T\mathbf{Q}$ (16)

2.3.4 Pole Placement Algorithm

\mathbf{F} is determined from solving the following equation

$$|s\mathbf{I} - \mathbf{A} + \mathbf{BF}| = (s - s_1)(s - s_2) \dots (s - s_n) \tag{17}$$

where $s_i (i = 1, 2, \dots, n)$ is chosen to be eigenvalues of matrix \mathbf{A} ; \mathbf{F} is chosen so that $|\mathbf{A} - \mathbf{BF}|$ having its eigenvalues will be s_i

3. NUMERICAL EXAMPLES

The 20-story structure used for this benchmark study were designed by Brandow and Johnston Associates 1996 for the SAC Phase II Steel Project [4]. These buildings were chosen because they also serve as benchmark structures for the SAC studies and, thus, will provide a wider basis for the comparison of results. All

simulations were performed by using routines written in MATLAB.

3.1 Description of the 20-Story Benchmark Structure

The 20-story structure made of steel with $E = 200GPa$. The modal damping ratios of the steel frame are $\zeta = 2\%$. The dynamic properties of structure are given in Table 1

Table 1: The dynamic properties of the 20-story structure

i th Floor	1 st	2 nd -4 th	5 th -10 th	11 st -13 rd
$k_i (kN/cm)$	30173	80400	51686	42295
$m_i (\times 10^3 kg)$	563	552	552	552
i th Floor	14 th -16 th	17 th -18 th	19 th	20 th
$k_i (kN/cm)$	27160	23917	16012	16012
$m_i (\times 10^3 kg)$	552	552	552	584

When the smart structure is not controlled, the first three natural frequencies corresponding to the first three mode are $\tilde{S}_1 = 7.1rad/s$; $\tilde{S}_2 = 18.2rad/s$; $\tilde{S}_3 = 30.3rad/s$ The first three time period of the structure are $T_1 = 0.88sec$; $T_2 = 0.34sec$; $T_3 = 0.21sec$. The viscous dampers coefficients of VFD (passive control) [3]: $C_i^{VFD} = 1.2 \times 10^6 (kN \cdot s/cm)$. For CSD and from the Century Spring manufacture, the stiffness of main springs of CSD (semi-active control) are taken as the maximum value of C_i^M an $x_{limit,i}^{f \text{ or } c}$ **Error! Reference source not found.:** $C_i^M = 46.62 (kN/cm)$. $x_{limit,i}^{f \text{ or } c} = 7.5 (cm)$. The response of the 20-story structure is computed for Northridge seismic excitation.

3.2 The dynamic response and the reductions of the structure using four algorithms

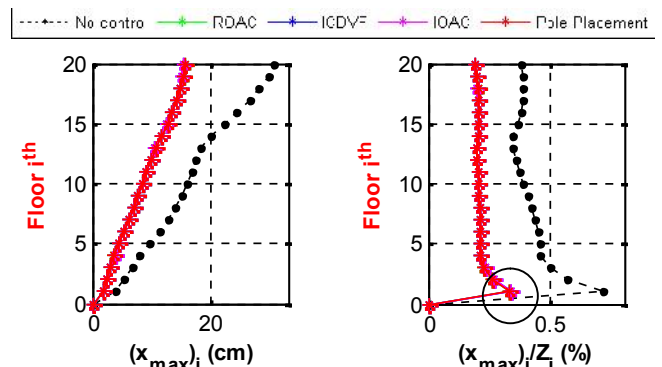


Fig 5: The maximum displacement response at the floors

Fig 6: The maximum shear force response relative to the height at the floors

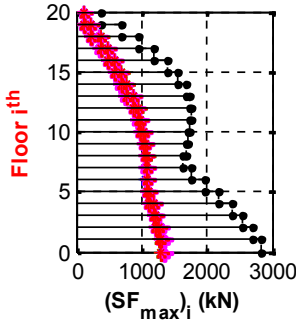


Fig 7: The maximum shear force response at the floors

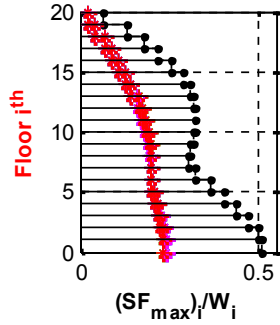


Fig 8: The maximum shear force response relative to the weight at the floors

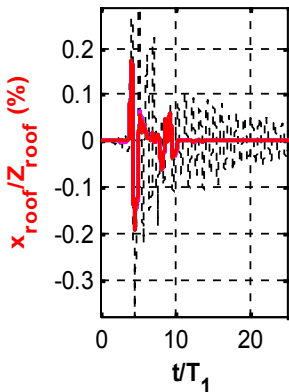


Fig 9: The roof displacement time history

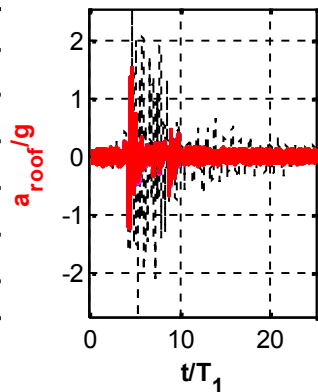


Fig 10: The roof acceleration time history

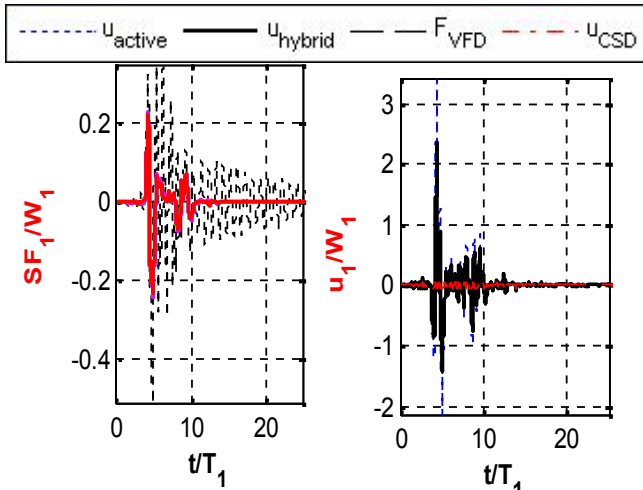


Fig 11: The 1st floor shear force time history

Fig 12: The 1st floor controlled force time history with IOAC

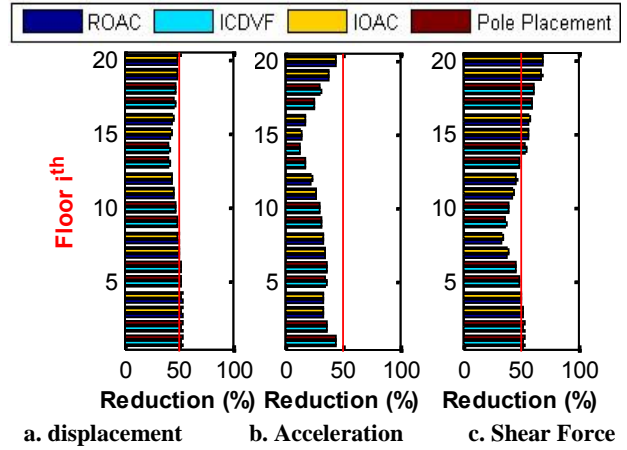


Fig 13: The maximum reduction

The responses of the structure using the four active control algorithms in charge of controlling the CSDs product are almost similar (from the Fig 5 to the

Fig 13). There is not much difference in the responses among these algorithms. Furthermore, retrofitted with the hybrid control system, the structure has the maximum ratio of x_{roof} to Z_{roof} (relative-to-ground level of 80.73m) which is only 0.17% and less than the Vietnam standard ratio of $1/500=0.2\%$ (according to the Vietnam code for tall buildings) (Fig 9). Whereas without the dampers, this ratio is 0.29% and exceeds the allowance value. Additionally, the hybrid structural control also reduces the 1st floor's deviation ($(x_{max})_i/Z_1$) (Fig 6) which is the main reason for the collapse of the building. In effort to reduces without using damper, the column's stiffness at the 1st floor is enhanced up to 4 times.

For this reason, hybrid control is appropriate to improving the seismic resistance of used buildings which must meet the requirements of seismic design's Vietnam code. Nevertheless, the maximum ratio of a_{roof} to g (the gravity acceleration, take $9.81m/s^2$) of the hybrid structure is equal to 1.53 and larger than the Vietnam standard ratio of 0.1. Ultimately, the hybrid control does not satisfy the impulse of the active control force (due to the capacity in generating control force of both VFD and CSD) (Fig 12), but the maximum reduction is approximately 50%.

3.3 The effectiveness of the response reduction of the hybrid control structure with only VFD and CSD

The response of the 20-story building with respect to the above specified seismic excitations is checked for the following five cases such as (A) uncontrolled structure; (B) passive control only VFD of $C_i^{VFD} = 1.2 \times 10^6 (kN.s/cm)$; (C) semi-active control only CSD of $C_i^M = 46.62 (kN/cm)$ and $x_{1limit,i}^{t or c} = 7.5 (cm)$ using IOAC; (D) hybrid control both the VFD and CSD with IOAC.

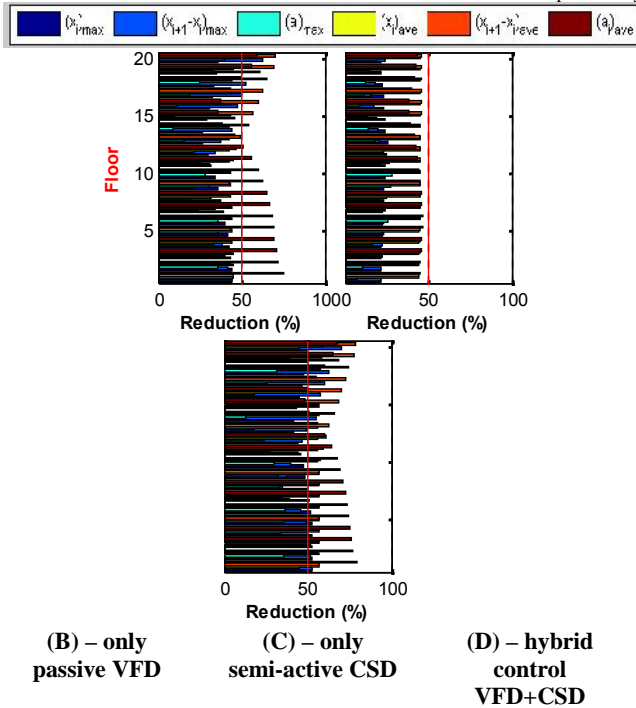


Fig 14: The response reduction of the structure

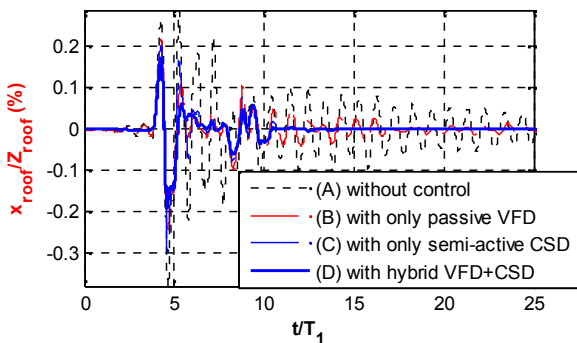


Fig 15: The roof displacement time history at the top floor

The criteria in attempts to assess the effectiveness in these cases (B), (C), and (D) is the response reduction R_{mean} and is computed by

$$R_{mean} = \frac{2 \times R_{max}^{mean} + R_{ave}^{mean}}{3} \quad (18)$$

Where
$$R_{max}^{mean} = \frac{1}{n} \sum_{i=1}^{n=20} \left[\frac{R_{(x_i)_{max}} + R_{(x_{i+1}-x_i)_{max}} + R_{(a_i)_{max}}}{3} \right];$$

$R_{(x_i)_{max}}$, $R_{(x_{i+1}-x_i)_{max}}$, and $R_{(a_i)_{max}}$ is the maximum and average displacement, relative displacement, and acceleration reductions compared with the no control case at the floors, respectively. The average responses are calculated with the root mean square value. The significance of the maximum response is taken into account in the expression (18) with scale factor of 2.

Table 2: The response reduction in three cases (B), (C), (D)

CASE	$\frac{1}{n} \sum_{i=1}^{n=20} R_{(x_i)_{max}}$	$\frac{1}{n} \sum_{i=1}^{n=20} R_{(x_{i+1}-x_i)_{max}}$	$\frac{1}{n} \sum_{i=1}^{n=20} R_{(a_i)_{max}}$	R_{max}^{mean}
(B)	35.6%	39.5%	27.7%	34.2%
(C)	22.9%	20.9%	18.0%	20.6%
(D)	48.3%	51.2%	30.4%	43.3%
	$\frac{1}{n} \sum_{i=1}^{n=20} R_{(x_i)_{ave}}$	$\frac{1}{n} \sum_{i=1}^{n=20} R_{(x_{i+1}-x_i)_{ave}}$	$\frac{1}{n} \sum_{i=1}^{n=20} R_{(a_i)_{ave}}$	R_{ave}^{mean}
(B)	43.8%	50.7%	57.6%	50.7%
(C)	44.8%	45.3%	43.3%	44.5%
(D)	56.9%	62.8%	65.7%	61.8%

Among these cases, the case (D) gives the best reduction, $R_{mean} = 49.5\%$, the case (B) has $R_{mean} = 39.7\%$ and the case (C) has $R_{mean} = 28.6\%$ (

Table 2). R_{mean} of the case (B) (passive control) is even larger than that of the case (C) (semi-active control). This results from the small capability of both C_i^M and $x_{limit,i}$ used with the maximum values. CSDs are therefore not able to product the significant control force to reduce the structure responses. In order to increase the response reduction, the number of CSD used in the structure should be adequate to the demand of semi-active control force. In addition, the CSD is very useful to eliminate the small vibration from $t/T_1 = 12$ to 25 (

Fig 15) and this is not true in the case (B). Lastly, for the smart structure, the combination of VFD and CSD {1} utilizes VFD's capability for generating control force to make up for lack of CSD's semi-active control force and (2) dismisses the small vibration phrase.

3.4 The effectiveness of response reductions of the hybrid structure with the classical solution

To investigate the effectiveness of response reductions of the structure, simulations were carried out on two solutions consisting of (D) using the hybrid control (VFD+CSD) and (E) four times of increasing the column's stiffness of structure (the stiffness of floors is calculated with (5))

Table 3: Column section property type of each solution, wide flange section

i th floor	Solution (D)		Solution (E)	
	property type	Section A (cm ²)	property type	Section A (cm ²)
1	W24x335	634.8	W36x848	1,225.8
2	W24x335	634.8	W36x848	1,225.8
3	W24x335	634.8	W36x848	1,225.8
4	W24x335	634.8	W36x848	1,225.8
5	W24x229	433.5	W30x526	993.5
6	W24x229	433.5	W30x526	993.5
7	W24x229	433.5	W30x526	993.5
8	W24x229	433.5	W30x526	993.5
9	W24x229	433.5	W30x526	993.5

i th floor	Solution (D)		Solution (E)	
	property type	Section A (cm ²)	property type	Section A (cm ²)
10	W24x229	433.5	W30x526	993.5
11	W24x192	363.2	W27x539	1,019.4
12	W24x192	363.2	W27x539	1,019.4
13	W24x192	363.2	W27x539	1,019.4
14	W24x131	248.4	W24x450	851.6
15	W24x131	248.4	W24x450	851.6
16	W24x131	248.4	W24x450	851.6
17	W24x117	221.9	W24x408	767.7
18	W24x117	221.9	W24x408	767.7
19	W24x84	159.4	W24x279	529.0
20	W24x84	159.4	W24x279	529.0
		7,737.6		19,070.6

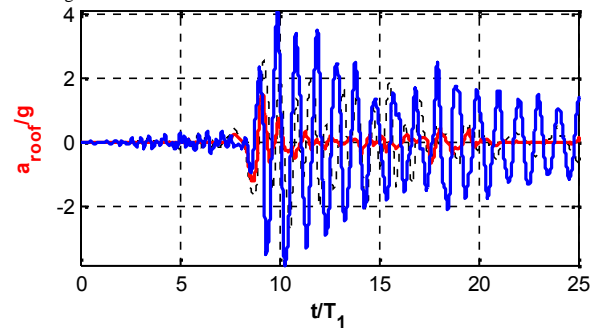


Fig 18: The roof acceleration time history

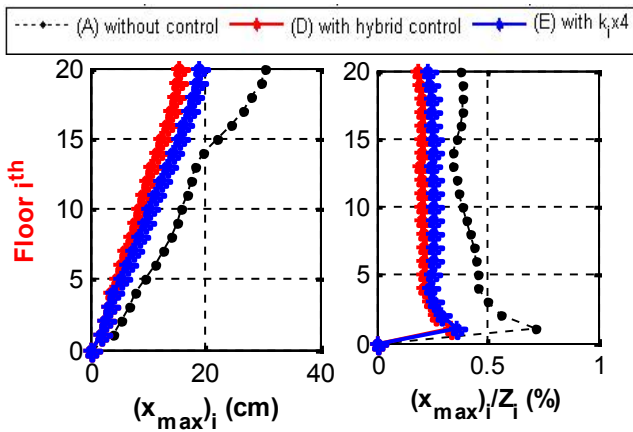


Fig 16: The maximum displacement response at the floors

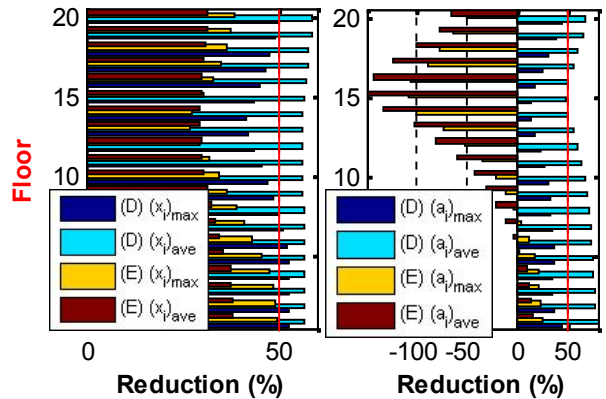


Fig 19: The maximum displacement reduction

Fig 20: The maximum acceleration reduction

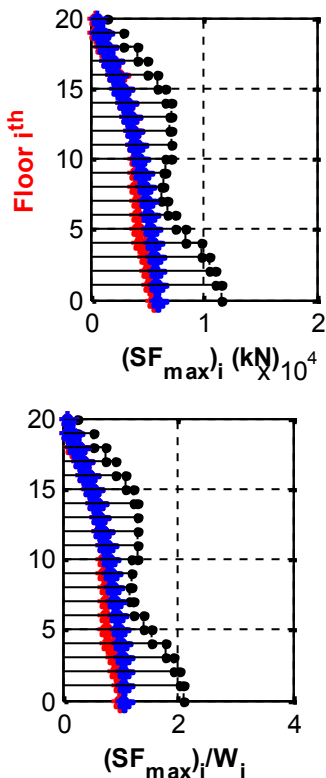


Fig 17: The maximum shear force response at the floors

As the columns' stiffness of the structure increase four times, the displacement are also enhanced, corresponding to the column's stiffness (Fig 16 and Fig 19). However, the acceleration response

reduction is negative (Fig 20), i.e. causing higher acceleration because the structure becomes stiffer. Additionally, the maximum shear force responses of (D) and (E) are nearly familiar (Fig 17), but in order to get amount of the reduction, the columns' stiffness of the structure in the case (E) must be four times increase. That means the steel material used for this building must

upgrade, up to $\frac{19,070.6}{7,737.6} = 2.46$ times, i.e. the costs for

the material are lessened of approximately 59.4 percent when the structure uses the hybrid controlled system.

4. CONCLUSION

As a hybrid control system, the 20-story structure is either the passive control with VFD or the semi-active control with CSD. Therefore, the hybrid control system with (VFD+CSD) is suitable for variety kinds of seismic loadings. Furthermore, when CSD uses an active control algorithm for the controller, this paper shows that all of the four active algorithms give the almost same responses. As structures are equipped with (VFD+CSD), the energy dissipation of system is principally the task of VFD. Yet, with the same main spring stiffness and CSD used as semi-a active control device, the response reduction develops effectiveness. The article also displays that the hybrid control system in

<http://www.ejournalofscience.org>

the 20-story building has more advantages for the seismic resistance than a traditional solution such as lowering a great amount of the material or not increasing the acceleration response for the structure. Besides, this research introduces an option for structural control, the hybrid control. To lessen costly consumption during operation and maintenance of using CSD and VFD simultaneously but the structure obtains desired effectiveness, the hybrid control system (VFD+CSD) is one of the optimal choices. Eventually, a hybrid control system with (VFD+CSD) in high-rise building becomes suitable for Vietnam condition being on the medium earthquake domain.

REFERENCES

- [1] Meirovitch. L, "Dynamics and Control of Structures", John Wiley & Sons, New York, 1990.
- [2] Anil K.Chopra, "Dynamics of Structures", 4th edition, Prentice Hall Press, 2012.
- [3] Robert J. Mcnamara and Douglas P. Taylor, "Fluid viscous dampers for high-rise buildings", the structural design of tall and special buildings, 12, 145–154, 2003.

- [4] Y.Ohtori, R. E. Christenson, B. F. Spencer, "Benchmark Control Problems for Seismically Excited Nonlinear Buildings", Journal of Engineering Mechanics © ASCE / April 2004.
- [5] Y. Ribakov, "Semi-Active predictive control of nonlinear structures with controlled stiffness devices and friction dampers", Structural design Tall Special Buildings 13, pp. 165-178, 2004.
- [6] <http://www.centuryspring.com/>

AUTHOR PROFILES

PHAM NHAN HOA received the master degree in civil engineering from Liege, Belgium in 2006. Currently, he is now a lecturer at International University – Vietnam National University, Vietnam.

CHU QUOC THANG received the PhD degree in structural engineering from TTI, Hungary in 1987. Currently, he is an Associate Professor at International University – Vietnam National University, Vietnam.